Optimizing MT Point Selections for Knee qMT as a First Step in Evaluating the Tibiofemoral Joint

Nade Sritanyaratana[1], Pouria Mossahebi[1], Alexey Samsonov[2], Kevin Johnson[3], Walter Block[1,3], and Richard Kijowski[2]

[1]*Biomedical Engineering, University of Wisconsin-Madison, Madison, WI, United States,* [2]*Radiology, University of Wisconsin-Madison, Madison, WI, United States,* [3]*Medical Physics, University of Wisconsin-Madison, Madison, WI, United States*

Purpose Quantitative Magnetization Transfer (qMT) exploits the magnetization transfer (MT) effect to provide a quantitative measure of macromolecular properties of articular cartilage. qMT parameters have been shown to correlate with macromolecular content in ex-vivo cartilage samples [1, 2] and to change with age and activity level within human patellar cartilage in-vivo [3]. qMT protocols utilize multiple magnetization transfer (MT) acquisitions with different combinations of offset frequencies and flip angles. In previous cartilage studies, qMT protocols sampled a wide range of offset frequencies and/or flip angles which resulted in long acquisition times and limited anatomic joint coverage. One way to decrease scan time is to optimize selection of these MT combinations in order to create a qMT protocol that can capture similar information with fewer acquisitions. The non-linear nature of the model makes it difficult to intuitively select optimal MT "points". In this study, we performed digital simulations to quantitatively choose the best MT combinations out of an array of offset frequencies and flip angles, determine an 8 "point" and a 4 "point" protocol that provide the most precision and accuracy in qMT parameters, and use these protocols to provide greater lateral coverage of the in-vivo weight-bearing surfaces of the tibiofemoral joint.

Methods *Digital simulations:* Digital simulations (See Figure 1) can be performed to determine an optimal qMT protocol for typical qMT values of articular cartilage. The qMT cross-relaxation model as proposed by Yarnkykh [4] and later modified by Mossahebi [5] can be solved numerically in the forward direction (Figure 1) using qMT parameters (f, k, T_{2b}), and other tissue parameters (proton density and $R_1=1/T_1$) to obtain raw MT signals of desired MT flip angles and offset frequencies (Δ). qMT parameters can also be solved iteratively in the backward direction (Figure 1), using a non-linear least squares algorithm. To obtain preliminary information about qMT values, we measured qMT parameters (f=12.5%, k=5.4, and T_{2b}=6.56μs) of patellar cartilage in 10 volunteers using a previous 8 point protocol [6], hereby named *Protocol 1*, at different MT offset frequencies and flip angles: 0.8/1550, 2.5/1550, 5/1550, 10/1550, 20/1550, .8/890, 2.5/890, 5/890 [kHz/°]. Based on these mean qMT values, raw MT signals of desired MT offsets and flip angles were calculated in the forward direction. Normally distributed noise was then added to the raw signals for an SNR of 75 in the MT "off" signal. The signals were then fit in the backward direction to obtain simulated human knee qMT values (f_{sim}, k_{sim}, T_{2b_sim}). A measure of parameter-to-noise ratio was calculated: $PNR_{param} = \frac{median(param_{sim})}{SD(param_{sim})}$, $param: \{f, k, T_{2b}\}$. An iterative simulation similar to the scheme proposed by Ives [7] was performed using offset frequencies from 2 to 20kHz (in 500Hz increments) and flip angles from 500° to 1550° (in 50° increments). Based on this simulation, 8 MT points that maximized the PNR were selected: 2/1550, 20/1550, 17/1450, 18/1350, 2/750, 5/750, 4/700, 2/600 [kHz/°], hereby referred to as *Protocol 2*. This combination was then used in a further simulation observing the PNRs in all possible 4 point combinations to obtain the best 4 point subset: 2/1550, 20/1550, 2/750, 5/750 [kHz/°], hereby referred to as *Protocol 3*. The PNRs were also compared to two protocols used in previous qMT studies involving ex-vivo human patellar cartilage, as referred to as *Protocols 4 and 5* [2], using the qMT values measured in the previous study, fixing T2b to 8μs as did the previous study, and maintaining the SNR for comparison.

Figure 1. The below schemes are essential in conducting a brute force Monte Carlo qMT optimization routine. The forward block is utilized to digitally create raw MT signals for different MT offsets (Δ) and flip angles. Varying noise can be added, and the backward block can be used to measure parameter-to-noise (PNR). The end goal is to maximize the PNR with an optimal set of MT offsets and flip angles.

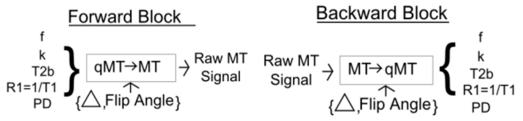

Table 1. PNR/TERs of digital phantom simulations.

Protocol	PNR_f	PNR_k	PNR_{T2b}	sum(PNR)
1. 8 pts in [6]	15.2	2.44	17.8	35.4
2. Proposed 8 pts	21.2	2.58	24.7	48.6
3. Proposed 4 pts	15.1	2.05	17.3	34.4
4. 27 pts in [2]	12.2	3.72	Fixed	(Fixed T2b)
5. 4 pts in [2]	6.60	.282	Fixed	(Fixed T2b)

Table 2. In-vivo PNRs.

Protocol	PNR_f	PNR_k	PNR_{T2b}	PNR
1. 8 pts in [6]	10.9	3.62	13.6	28.2
2. Proposed 8 pt	24.3	3.76	17.8	45.9
3. Proposed 4 pt	15.8	3.59	12.1	31.5

In-vivo experiments: The quality of the protocols was tested in in-vivo patella. The knee joint of one volunteer was imaged using *Protocols 1, 2, and 3* with each scan acquired twice to obtain in-vivo measures of patellar cartilage PNR. To validate the consistency of *Protocol 3* (4 point protocol) compared to *Protocol 2* (8 point protocol), the knee joint of one subject was imaged in the axial plane using *Protocols 2* and *3*. For both protocols, qMT parameters were solved in the backward model and then correlated on a point-by-point basis within an ROI covering the entire patellar cartilage. Lastly, the knee joint of one volunteer was imaged using Protocol 3 in the sagittal plane covering the central portion of the tibiofemoral joint in a 30 minute scan time. Just like the previous axial qMT protocol, each MT acquisition utilized a t_m=18ms, TR=42ms, TE=3.5ms, 14 cm FOV, 256 x 256 matrix, and 4 mm slice thickness. Because the qMT model requires knowledge of B_1 and T_1, additional acquisitions were also acquired for an AFI and VFA fitting [8, 9]. The signals were then solved in the backward direction to acquire f, k, and T_{2b} cartilage maps of human tibiofemoral joint.

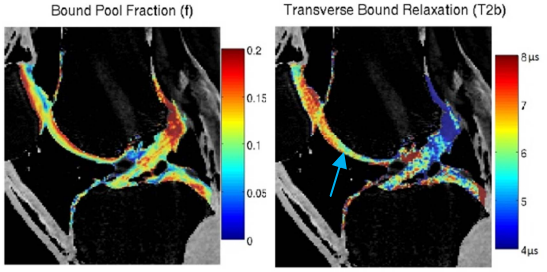

Figure 2. Sagittal f map of knee joint shows depth dependent variations of f values in patellar and trochlear cartilage. Corresponding sagittal T_{2b} map shows absence of magic angle effect on T_{2b} values of trochlear cartilage (arrow).

Results The PNRs for the digital simulations for *Protocols 1-5* are shown on Table 1, and PNRs from imaging human patellar cartilage in-vivo using *Protocols 1-3* are shown in Table 2. Point by point correlations in qMT values for human patellar cartilage between *Protocols 2* and *3* showed the following Pearson R correlation coefficients: R_f = 0.988, R_k = 0.852, R_{T2b} = 0.905, R_{PD} = 0.999, R_{R1} = 0.999. qMT images for one slice covering the tibiofemoral condyle are shown in Figure 1. A depth-dependent variation in f can be observed in the patellar cartilage, as well as in the tibiofemoral condyle.

Discussion The digital simulations provide a way to improve qMT parameter quality and have been validated on human patellar cartilage in-vivo. The simulated PNR between protocols seem to align according to the measured PNR calculations, and the proposed 4 point protocol provides comparable performance to the 8 point protocol from [6]. The protocols from previous ex-vivo studies [1] show lower PNRs (except for PNR_k in *Protocol 4*) possibly because the previous study utilized lower resolutions and likely longer acquisition times in order to maximize SNR. Our study shows that an abbreviated optimized 4-point protocol can provide similar qMT values within patellar cartilage as an optimized 8-point protocol. The reduced scan time makes it more feasible to image the entire knee joint in the sagittal plane, thereby allowing researchers to measure qMT values within both the patellofemoral and tibiofemoral compartment of the knee joint in-vivo.

References [1] Stikov, N. MRM, 2011. [2] Henkelman, R. MRM, 2002. [3] Sritanyaratana N. ISMRM abstract #1382, 2012. [4] Yarnykh, V. Neuroimage, 2004. [5] Mossahebi P. ISMRM abstract #0741, 2012. [6] Kijowski R. ISS abstract #3, 2012. [7] Levesque I. MRM, 2011. [8] Yarnykh, V. MRM, 2007. [9] Deoni S. MRM, 2003.

Acknowledgements We acknowledge the support of NIH NIAMS U01 AR059514-03 and GE Healthcare for making this research possible.